Published in final edited form as:
Am J Physiol Heart Circ Physiol. 2002 August ; 283(2): H741–H749. doi:10.1152/ajpheart.00096.2002.

Initiation and propagation of ectopic waves: insights from an in vitro model of ischemia-reperfusion injury

Ara Arutunyan, **Luther M. Swift**, and **Narine Sarvazyan**
Department of Physiology, Texas Tech University Health Sciences Center, Lubbock, Texas 79430

Abstract

The objective of the present study was to directly visualize ectopic activity associated with ischemia-reperfusion and its progression to arrhythmia. To accomplish this goal, we employed a two-dimensional network of neonatal rat cardiomyocytes and a recently developed model of localized ischemia-reperfusion. Washout of the ischemia-like solution resulted in tachyarrhythmic episodes lasting 15–200 s. These episodes were preceded by the appearance of multiple ectopic sources and propagation of ectopic activity along the border of the former ischemic zone. The ectopic sources exhibited a slow rise in diastolic calcium, which disappeared upon return to the original pacing pattern. Border zone propagation of ectopic activity was followed by its escape into the surrounding control network, generating arrhythmias. Together, these observations suggest that upon reperfusion, a distinct layer, which consists of ectopically active, poorly coupled cells, is formed transiently over an injured area. Despite being neighbored by a conductive and excitable tissue, this transient functional layer is capable of sustaining autonomous waves and serving as a special conductive medium through which ectopic activity can propagate before spreading into the surrounding healthy tissue.

Keywords

cultured myocytes; calcium transients; ischemic border zone

Cardiac arrhythmias arise from abnormalities of either impulse propagation (reentry based) or impulse initiation (focal or ectopic). Although the development of reentry arrhythmias, which involves rotation of an excitation wave around an anatomic or functional block, is conceptually well understood (19,34,44), it remains unclear exactly how the excitation propagates from an ectopic cell into the surrounding cell network. Previous studies have addressed several important questions about ectopic activity associated with ischemia-reperfusion. Specifically, many electrophysiological studies have shown the ability of individual myocytes to exhibit either triggered activity or abnormal automaticity upon reperfusion and have tied such arrhythmic behavior to specific ionic currents (7,11,54). Studies conducted in isolated papillary muscles and Purkinje fibers have revealed the importance of electrotonic interactions across inexcitable regions of tissue in modulating the activity of ectopic foci (1) and the role of entrance block with exit conduction (protected ectopic foci) for depolarization-induced automaticity to spread (31,41). Mapping studies conducted in intact hearts have revealed that 25% and 75% of arrhythmias occurring during ischemia and reperfusion, respectively, can be traced to ectopic sources (37), with the

Address for reprint requests and other correspondence: N. Sarvazyan, Dept. of Physiology, Texas Tech Univ. Health Sciences Center, 3601 Fourth St., Lubbock, TX 79430 (Narine.Sarvazyan@ttmc.ttuhsc.edu).

majority located close to the ischemic border zone (20). Finally, theoretical studies have addressed the critical size of an automatic focus, the safety factor (ratio of generated charge and that required to excite neighboring cells), and the roles of cell-to-cell coupling and anisotropic conduction in the propagation of ectopic activity (21,43,49). Despite these significant advancements, the actual progression of ectopic activity to arrhythmia has yet to be observed, mainly because the ischemic border of intact cardiac tissue has been inaccessible to real-time observation on a cellular scale. To visualize such a progression, we used a cellular model of ischemia-reperfusion that was recently developed in our laboratory (2). The results we obtained with this model not only have substantiated earlier theoretical estimates of the critical size of ectopic loci and the role of uncoupling in the generation of ectopic activity, but have also revealed a new phenomenon: a transient functional layer that is capable of sustaining autonomous ectopic waves.

MATERIALS AND METHODS

Myocyte cultures

Cardiomyocytes from 1- and 2-day-old Sprague-Dawley rats were obtained by an enzymatic digestion procedure described previously (2). The cells were plated on 25-mm laminin-coated glass coverslips (10^5 cells/cm^2) and kept under standard culture conditions in DMEM, supplemented with 5% fetal bovine serum (FBS), 10 U/ml penicillin, 10 μg/ml gentamicin, and 1 μg/ml streptomycin. By the third day in culture, the cells had formed interconnected confluent networks that exhibited rhythmic, spontaneous contractions. The cells were used in experiments for the next 3–4 days.

Intracellular calcium measurements

Cells were loaded for 1 h with 5 μM fluo 4-AM in Tyrode solution at room temperature. The superfusion solutions contained 0.25 μM fluo 4-AM to maintain the intracellular dye concentration during extended experiments. Each spontaneous or stimulated action potential was associated with a transient increase in intracellular calcium (Ca_i^{2+}), which we observed as a fluo 4 transient. To estimate diastolic slope values, we calculated Ca_i^{2+} using the following equation (17): $Ca_i^{2+}=K_dR/(K_d/[Ca_{rest}^{2+}]-R+1)$, where R is the normalized fluorescence (F/F_0), F_0 is the fluo 4 fluorescence at rest, and K_d is the dissociation constant for the Ca^{2+}-fluo 4 complex. A value of 0.345 μM was assumed for the K_d (15), and resting Ca_i^{2+} (Ca_{rest}^{2+}) was assumed to be 100 nM (10). The rate of change of Ca_i^{2+} during 0.5 s preceding the fast rising phase of the Ca_i^{2+} transient (CaT) was determined by linear regression. To visualize the propagation of ectopic activity, we recorded CaT instead of membrane potentials due to the following technical reasons. First, the closed design of the local injury chamber, which was essential for the temporal and spatial stability of the injury zone (I-zone) (2), precluded direct access by an electrode. Second, voltage-sensitive dyes exhibit less than a 10% change of emission intensity in response to an action potential (compared with a 10-fold increase in fluo 4 intensity associated with a CaT). This limited dynamic range renders potentiometric indicators unsuitable for experiments that require low magnification objectives to visualize the unpredictable occurrence of ectopic foci in a two-dimensional multicellular network, because these objectives collect only a limited amount of emitted light due to their low numerical apertures. In addition, rapid photobleaching of potentiometric dyes makes them inappropriate for extended experiments (40).

Experimental chamber

The experimental chamber consisted of a stainless steel holder for mounting a glass coverslip and a Plexiglas base that contained two inlets and one outlet (2). Inflow rates for

the injury (I-solution) and control solutions (C-solution) were 30 and 75 μl/min, respectively. Two platinum electrodes embedded in the top of the chamber were used to stimulate a small cluster of myocytes immediately below. This stimulation initiated a wave of CaT that spread throughout the rest of the network with a propagation velocity of 6–9 cm/s. To determine the excitation threshold, we applied monophasic 1.2-ms pulses starting at 0.4 V/cm and then increased the stimuli in 0.1-V increments until each pacing pulse was followed by a CaT wave. The monolayer, which behaved as a syncytium, was then continuously paced at 0.2–0.5 Hz by a voltage 20% higher than the excitation threshold (average threshold values were 0.8 V/cm). Although we were able to observe reperfusion arrhythmias at 37°C, the temporal resolution of CaT recordings decreased substantially at this temperature. Consequently, we conducted the experiments at 25°C by mounting the stainless steel holder in a microincubator (Medical Systems) equipped with a Peltier controller, which provided a constant temperature inside the chamber. We chose not to employ a lower temperature, because of a decrease in gap junctional permeability, which occurs at temperatures below 20°C (8).

Experimental protocols

All solutions, including the I-solution, were equilibrated with atmospheric oxygen. The experiments were conduced in either spontaneously beating or paced (if intrinsic frequency was <0.1 Hz) monolayers. Initially, cells were superfused for 10–20 min with a control Tyrode solution containing (in mM) 136 NaCl, 0.8 $MgCl_2$, 4.0 KCl, 1.2 $CaCl_2$, 5.6 glucose, and 10 HEPES; pH 7.3. Subsequently, within 15 s after the onset of I-solution, an I-zone was created as described previously (2). This I-zone was surrounded by a control zone (C-zone), which was composed of myocytes superfused by control Tyrode solution. Washout with the control Tyrode solution constituted “reperfusion.” The “microreperfusion” protocol was accomplished by substituting a washout step with increased relative inflow rates for the C- and I-solutions. Specifically, flow from a 5-ml syringe was added in parallel to flow from the control 30-ml syringe. This increased the flow of C-solution from 75 to 90 μl/min (while inflow of the I-solution remained the same) and effectively reduced the size of the I-zone.

Injury solution

The terms “ischemic” or “injury” environment in our study refer to a solution that reproduces certain elements of the extracellular milieu of ischemic cells (2,48). It consisted of (in mM) 136 NaCl, 0.8 $MgCl_2$, 8 KCl, 1.2 $CaCl_2$, 20 deoxyglucose, 2 heptanol, 5 HEPES, and 5 MES; pH 6.5. Inclusion of the gap junction uncoupler heptanol allowed us to mimic the uncoupling effects of free fatty acids, e.g., arachidonic and palmitoleic acids, which have been shown to accumulate in the extracellular milieu of ischemic tissue (12,38). In neonatal rat cardiomyocytes, 2 mM heptanol reversibly inhibits gap junction permeability (6,46), whereas it’s effect on Ca_i^{2+} and spontaneous contractions is negligible (4,23).

Acquisition systems

Fluo 4-loaded cells were imaged with low power magnification objectives (Olympus PlanApo ×2/0.08 numerical aperture and UPlanFl ×10/0.3 numerical aperture) to capture the I- and C-zones simultaneously. For the experiments shown in Figs. 1, 2, 4, and 5, the BioRad MRC 1024 confocal system was used. Experiments presented in Fig. 3 were acquired with a Metafluor Imaging System equipped with an intensified charge-coupled device camera (Pentamax, Princeton Instruments).

Data analysis

Unless specified otherwise, the conclusions of this study were based on the analysis of over 300 injury/reperfusion episodes (yield from a single litter was sufficient to plate 20–40

coverslips, which were then used for individual experiments). Specifically, in 190 experiments with the I-solution containing heptanol, the following responses were obtained: *1*) no changes (immediate return to the original frequency), 46 cases (24%); and *2*) tachyarrhythmias, 144 cases (76%). Tachyarrhythmias, in turn, included *1*) tachycardia (monotonic increase in frequency), 57 cases (30%); *2*) arrhythmia (irregular increase in frequency with observable ectopic beats), 63 cases (33%); and *3*) tachyarrhythmia associated with the formation of spiral waves, 24 cases (13%). Spirals and other spatiotemporal patterns, which formed as a result of colliding ectopic waves, will be the subject of a followup paper and thus are not discussed here. In the 120 experiments that employed heptanol-free I-solution, tachycardia was observed 13 times (11%) and arrhythmia with the ectopic extra beats was observed 6 times (5%). The presented figures are typical results of corresponding scenarios. Quantitative results are expressed as means ± SD. Data and images were plotted using Microcal Origin 6.0 and Scion (NIH) Image software.

Chemicals

Collagenase type II was obtained from Worthington (Freehold, NJ). Media and porcine trypsin were obtained from GIBCO-BRL (Grand Island, NY). Fluo 4-AM was purchased from Molecular Probes (Eugene, OR). FBS and all other chemicals were purchased from Sigma (St. Louis, MO).

RESULTS

Appearance of ectopic clusters

During “ischemia,” the amplitude of CaTs within the I-zone declined progressively and was followed by cessation of cell beating. Although changes in CaT frequency inside and outside the I-zone were not detected during perfusion with I-solution, tachyarrhythmic episodes lasting 15–200 s were recorded in both the C- and I-zones immediately upon restoration of control flow in ~76% of the experiments. When these tachyarrhythmic episodes occurred, we observed ectopic CaTs within the former I-zone, predominantly within or close to the border (Fig. 1). Such ectopic activity appeared as a local increase in Ca_i^{2+} with the amplitude and duration similar to pacing-elicited CaTs (Figs. 1 and 2). The average distance from the center of the functional border (defined in Ref. 2) to an ectopic cluster was 232 ± 113 μm. The linear sizes of the observed ectopic clusters varied from 180 to 300 μm (236 ± 57 μm), encompassing ~2–9 × 10^4 μm^2 (shape of ectopic clusters depended on particular cellular arrangement, see examples in Figs. 1 and 2). This area corresponds to ~8–50 cells, which is in agreement with theoretical studies that estimate the minimum size of the ectopic region as 8–10 cells (52). It is possible, however, that these numbers are overestimates, because high binning, which was used to acquire the images, lowers spatial resolution of images to 44 μm/pixel (×2 objective) and makes clusters smaller than ~100 μm indistinguishable from noise. The fate of ectopic clusters was threefold: *1*) activity remained confined to the ectopic cluster and, after 1–3 ectopic beats, this area was “swept” by a CaT wave from another source; *2*) the cluster slowly expanded, encompassing a larger area of border or I-zone cells (Fig. 2, *B* and *C*) but failed to propagate into the control network; and *3*) slow (0.1–0.4 cm/s) expansion of the ectopic cluster caused excitation of the surrounding network with fast propagation velocities (Fig. 2, *C* and *D*). As a result of the above events, a complex pattern of colliding ectopic waves spread through the entire field, including the former I- and C-zones. The exact patterns varied between experiments.

Ectopic activity is associated with changes in CaT shape

To understand the basis of the elevated excitability of ectopic regions, we examined CaTs in more detail using the MetaFluor imaging system (Fig. 3). Specifically, recordings were

obtained from the border area and included CaTs from both ectopic and control regions. An immediate increase of baseline Ca_i^{2+} was observed in myocytes from the ectopic regions upon reperfusion (Fig. 3, red trace). In this particular experiment, the first ectopic beat (black arrow) failed to propagate to neighboring myocytes, but the next CaT from the same ectopic locus drove the cell network for at least 140 s, until the pace approached the initial frequency of the layer. The slowing of ectopic pacing during the later stages of reperfusion revealed an important feature of the ectopic cells' CaT, a prominent rise in diastolic Ca_i^{2+} (Fig. 3, red arrows), which resembled the diastolic depolarization of a pacemaker cell.

Although only an estimate of Ca_i^{2+} can be obtained from nonratiometric calcium probes, such as fluo 4, we calculated slope values for the control and ectopic CaTs using the K_d value of 345 nM (15,17). The slope in ectopic regions ranged from 7 to 40 nM/s and was significantly higher than in control traces (Fig. 3*C*). This slope disappeared upon return of the original pacing pattern, suggesting its direct involvement in ectopic activity.

Role of cell-to-cell coupling and the number of injury events

Omission of heptanol from the I-solution sharply reduced the incidence of reperfusion arrhythmias (from 76% to 16%). Thus a 10-min superfusion with uncoupler-free I-solution resulted in the return of CaTs and restoration of rhythmicity across the entire field in a majority of the experiments. However, if the 10-min ischemia/10-min reperfusion cycle was repeated, the occurrence of reperfusion arrhythmias increased in proportion to the number of injury events (Fig. 4*A*). Typical traces from the C- and I-zones during the repetitive injury protocol are shown in Fig. 4*B*, and tachyarrhythmic episodes are marked with an asterisk. The lower traces in Fig. 4 reveal that tachyarrhythmic episodes in the C-zone occurred when cells inside the I-zone failed to exhibit CaTs upon reperfusion.

Role of border zone propagation

Upon reperfusion, ectopic CaT often propagated along small areas of the border and then spread into the C- and recovering I-zones. In one series of experiments, we blocked the propagation of such activity into the inner area of the I-zone by continuing to superfuse it with I-solution (see MATERIALS AND METHODS and Fig. 5). Such "microreperfusion" allowed us to confine ectopic activity to the large segments of the border zone (Fig. 5*A*). Border zone propagation was followed by the escape of ectopic activity from the border zone into the surrounding control network, resulting in the generation of arrhythmias (Fig. 5*B*).

DISCUSSION

Despite recent advances in mapping electrical activity in the heart (35,45,47,55), cellular events within the border zone of an ischemic area have not been observed in situ. Thus until now the initial stages of ectopic activity and its propagation have been addressed mainly by computational approaches (16,21,52,53). In contrast, this study provides insights from direct observation of ectopic activity, resulting from a new experimental approach developed in our laboratory (2). It employs a multicellular network of myocytes and fluo 4 fluorescence to visualize propagating ectopic waves of CaTs. Despite the absence of electrophysiological measurements, the results are highly relevant to cardiac arrhythmias. First, ultimately it is the disorganized contraction (as a result of CaT), not electrical activity, that renders the heart unable to pump blood efficiently. Second, monitoring CaTs as a means to measure beat rates and the velocity of impulse propagation has been used successfully both in vitro and in vivo (5,14,24). Third, CaTs measured in our experiments were direct indications of propagating action potentials, because the velocity of CaT wave propagation exceeded by at least two orders of magnitude the velocity of diffusion-based Ca waves (25,27) and was similar to the velocity of action potentials measured by others in neonatal myocyte cultures (13,29). In

addition, the magnitude and velocity of ectopic CaTs that spread from the I-zone to the C-zone were identical to these elicited by the external pacing electrodes.

In our experimental protocol, the generation and propagation of ectopic activity occurred only during washout of the I-solution, i.e., during reperfusion (Figs. 1–3). What are the factors that promoted the generation of ectopic beats in these experiments? In the presence of I-solution, the gap junction conductance of myocyte within the I-zone is decreased due to the uncoupling effects of low pH (32,51) and heptanol (4,23,46). Although upon reperfusion heptanol is rapidly removed from the cell surroundings (<15 s), intercellular coupling was restored only gradually. For example, Bastide et al. (4) found that gap junction conductance in neonatal rat myocyte pairs was restored to 90% of its control value ~90 s after withdrawal of heptanol. Therefore, during the first 100 s of reperfusion, a range of coupling conductances is superimposed upon rapidly recovering cell excitability, which passes through abnormally high values during the initial phase of reperfusion (7,11,33). Thus the combination of high excitability and decreased intercellular coupling creates conditions that favor the generation and propagation of ectopic activity from an individual myocyte or myocyte cluster (42). By decreasing cell-to-cell coupling, one effectively reduces a current "sink" leading to improvement of impulse propagation from an active focus (21,50,52). A similar phenomenon, a paradoxical improvement in the safety factor of conduction, was observed when cell-to-cell coupling was reduced in branching strands of cardiomyocytes (39). Our experiments provided two lines of evidence that decreased cell-to-cell coupling is essential for the successful progression of ectopic activity. First, omission of heptanol from the I-solution reduced the occurrence of reperfusion arrhythmias by more than fourfold (from 76% to 16%), suggesting that elevated excitability, alone, is insufficient for ectopic activity to proceed. Importantly, heptanol-containing control Tyrode solution failed to cause reperfusion arrhythmias (data not shown). The second line of evidence comes from our repetitive injury experiments (Fig. 4). Although CaTs recovered after a single exposure to heptanol-free I-solution, repetitive injury progressively diminished CaT amplitudes (Fig. 4*B*) and eventually led to cell death within the I-zone, as assessed with trypan blue (data not shown). At the same time, a strong correlation was observed between the incidence of reperfusion arrhythmias and the absence of CaTs in the I-zone upon reperfusion (Fig. 4A). Thus we hypothesize that the irreversible injury of I-zone myocytes, which is induced by repetitive ischemia-reperfusion cycles, removed the I-zone as an effective current "sink" and increased the probability of ectopic beat generation from the border zone. In other words, repetitive injury creates a unidirectional block for border zone cells, thereby increasing the safety factor for successful propagation of ectopic beats (49).

Whereas diminished coupling appears to be essential for both the generation and propagation of ectopic activity, an additional factor, increased cell excitability, is required for an ectopic cell or cluster to emerge. Direct visualization of ectopic sources in our cellular model of reperfusion-ischemia injury allowed us to simultaneously observe CaTs in ectopic and control regions. The distinguishing characteristic of the ectopic regions was a slow increase in diastolic Ca_i^{2+}, which preceded the CaT and resembled the diastolic depolarization typical of pacemaker cells (Fig. 3). The basis of such an increase in diastolic Ca_i^{2+} is unknown. It could be the consequence of reperfusion-induced alterations of ion channels and transporters or from reperfusion-induced Ca^{2+} overload (7,9). The latter is known to occur in cardiac myocytes upon recovery from ischemia or acidosis and can cause triggered activity as a result of the inward sodium current generated by the Na^+/Ca^{2+} exchanger or Ca^{2+}-activated nonselective cation channels, facilitating myocyte depolarization. Ca^{2+} overload also enhances the probability of Ca^{2+} efflux from the sarcoplasmic reticulum (SR) during diastole, thereby increasing the likelihood of automaticity in latent pacemaker cells as well as ventricular and atrial myocytes (3).

Through a positive feedback loop, which involves low-voltage-activated T-type Ca^{2+} channels and Ca^{2+}-induced Ca^{2+} release from the SR, subsarcolemmal Ca^{2+} also may induce pacemaker activity in atrial cells (18,26). Any of these mechanisms could be involved in the slow rise of diastolic Ca_i^{2+} observed in our experiments.

In addition to the ionic basis of ectopic foci, it is important to understand how such activity is propagated. The fact that every myocyte within the recovering border zone was subjected to similar conditions in our experimental setup, and that multiple ectopic sites emerged upon reperfusion, suggest, that many, if not all, border cells are capable to exhibit ectopic activity. Thus assuming that the entire border zone area gains automaticity or triggered activity, we hypothesize that impulse propagation within such an area should follow the principles known for the sinoatrial (SA) node. In fact, theoretical studies have shown that thousands of pacemaker cells generate synchronized outgoing action potentials by an entrainment process in the SA node: after leading cell fires, an activation front propagates through the rest of the already entrained pacemakers with an apparent, slow conduction velocity (30). If such a tissue has homogeneous physiological properties, waves of action potentials generated from an ectopic source would be spread spherically. However, if the tissue surrounding the leading cell is not homogeneous with regard to either junction conductance or diastolic depolarization rate, the activation of neighboring cells would be asymmetric. Diastolic depolarization then acts as a “pulling” force, yielding in the extreme case a linear propagation. We observed such “linear” propagation along small (200–400 μm) regions of the border zone. The microreperfusion protocol allowed as to effectively “focus” ectopic activity in a narrow layer around the I-zone (Fig. 5).

Although we failed to observe ectopic activity during in vitro “ischemia,” 25% of the arrhythmias that occur during ischemia in vivo can be attributed to ectopic sources (36). How can one explain this apparent paradox? We suggest that ischemic process in vivo could be associated with conditions, which are similar to those in the microreperfusion protocol. Specifically, it could be due to the dynamic conditions associated with an infarct area, when metabolic vasodilatation of adjacent coronary beds transiently relieves ischemic conditions in small areas of the infarct’s border. Myocytes within such areas might then act as a source of ectopic arrhythmias, as we observed in our study. In other words, a microreperfusion-like process could be responsible for arrhythmias that occur during ischemia.

Whether initial development of ectopic activity occurred in small ectopic clusters during the original ischemia-reperfusion protocol or in an extended borderline pattern (microreperfusion protocol, Fig. 5), at this stage CaT spread with an apparent low velocity (0.1–0.4 cm/s). Such low velocities, nevertheless, exceed by at least order of magnitude the speed of Ca_i^{2+} waves caused by Ca^{2+}-induced Ca^{2+} release (22). On the other hand, the apparent velocities of CaTs in ectopic clusters were an order of magnitude slower than the propagation of CaTs through the control network (6–9 and 14–18 cm/s at 25 and 37°C, respectively). Thus we suggest that the slow velocities we observed in ectopic clusters were due to the entrainment mechanisms of conduction in a network of ectopically active cells, where the activation propagates with a slow apparent velocity (30).

On the basis of the results of the present study, one can extrapolate the concept of “border zone” propagation in a two-dimensional myocyte network to the three-dimensional myocardium by incorporating the following scenario of events. At the onset of global or partial reperfusion, reversibly injured cardiomyocytes form a transient functional layer over an infarcted, irreversibly injured area. Such a layer might consist of ectopically active but poorly coupled myocytes (“pacemaker-like layer”) that are capable of sustaining autonomous ectopic waves. Upon restoration of cell-to-cell coupling, these ectopic waves

would escape into the healthy network, generating arrhythmias. Given the significant differences in the electrical properties of cultured neonatal rat cardiomyocytes and adult human ventricular myocardium, additional experiments will be required to confirm occurrence and clinical relevance of such a scenario in vivo.

In summary, direct observation of reperfusion-induced ectopic activity in a two-dimensional network of neonatal rat cardiac myocytes corroborated theoretical predictions regarding the interplay between excitability and cell-to-cell coupling required for ectopic beat propagation. We have shown that an ectopic focus has to expand to a cell cluster of certain dimensions to activate the surrounding network. The experiments also revealed that CaTs in ectopic regions exhibit a slow rise during diastole and suggested that activity within an ectopic cluster propagates via a slow, entrainment-like process, similar to the propagation of action potentials in the SA node. Our results also suggest that, upon reperfusion, a functional ectopically active layer can be formed transiently over an injured area. Despite being surrounded by a normally conductive and excitable tissue, this layer, itself, can exhibit transient autonomous activity. These results may provide further insights into the mechanisms that underlie arrhythmias in the human myocardium.

Supplementary Material

Refer to Web version on PubMed Central for supplementary material.

Acknowledgments

The authors are indebted to Dr. Richard Nathan for editorial suggestions and Dr. Valentin Krinsky for valuable discussions. We also grateful to Drs. A. Escobar, A. Pertsov, and E. Holmuhamedov for comments on the manuscript.

This work was supported by the American Heart Association.

REFERENCES

1. Antzelevitch C, Jalife J, Moe GK. Electrotonic metabolism of pacemaker activity. Further biological and mathematical observations on the behavior of modulated parasystole. Circulation 1982;66:1225–1232. [PubMed: 7139901]
2. Arutunyan A, Webster DR, Swift LM, Sarvazyan N. Localized injury in cardiomyocyte network: a new experimental model of ischemia-reperfusion arrhythmias. Am J Physiol Heart Circ Physiol 2001;280:H1905–H1915. [PubMed: 11247808]
3. Bassani RA, Bassani JW, Lipsius SL, Bers DM. Diastolic SR Ca efflux in atrial pacemaker cells and Ca-overloaded myocytes. Am J Physiol Heart Circ Physiol 1997;273:H886–H892.
4. Bastide B, Herve JC, Cronier L, Deleze J. Rapid onset and calcium independence of the gap junction uncoupling induced by heptanol in cultured heart cells. Pflügers Arch 1995;429:386–393.
5. Bub G, Shrier A, Glass L. Spiral wave generation in heterogeneous excitable media. Phys Rev Lett 2002;88 058101.
6. Burt JM, Massey KD, Minnich BN. Uncoupling of cardiac cells by fatty acids: structure-activity relationships. Am J Physiol Cell Physiol 1991;260:C439–C448.
7. Carmeliet E. Cardiac ionic currents and acute ischemia: from channels to arrhythmias. Physiol Rev 1999;79:917–1017. [PubMed: 10390520]
8. Chen YH, DeHaan RL. Temperature dependence of embryonic cardiac gap junction conductance and channel kinetics. J Membr Biol 1993;136:125–134. [PubMed: 7508979]
9. Choi HS, Trafford AW, Orchard CH, Eisner DA. The effect of acidosis on systolic Ca^{2+} and sarcoplasmic reticulum calcium content in isolated rat ventricular myocytes. J Physiol 2000;529:661–668. [PubMed: 11118496]

10. Church DJ, Rebsamen MC, Morabito D, van Der Bent V, Vallotton MB, Lang U. Role of cell contractions in cAMP-induced cardiomyocyte atrial natriuretic peptide release. Am J Physiol Heart Circ Physiol 2000;278:H117–H125. [PubMed: 10644591]
11. Cordeiro JM, Howlett SE, Ferrier GR. Simulated ischaemia and reperfusion in isolated guinea pig ventricular myocytes. Cardiovasc Res 1994;28:1794–1802. [PubMed: 7867032]
12. Dhein S, Krusemann K, Schaefer T. Effects of the gap junction uncoupler palmitoleic acid on the activation and repolarization wavefronts in isolated rabbit hearts. Br J Pharmacol 1999;128:1375–1384. [PubMed: 10602315]
13. Entcheva E, Lu SN, Troppman RH, Sharma V, Tung L. Contact fluorescence imaging of reentry in monolayers of cultured neonatal rat ventricular myocytes. J Cardiovasc Electrophysiol 2000;11:665–676. [PubMed: 10868740]
14. Fast VG, Ideker RE. Simultaneous optical mapping of transmembrane potential and intracellular calcium in myocyte cultures. J Cardiovasc Electrophysiol 2000;11:547–556. [PubMed: 10826934]
15. Gee KR, Brown KA, Chen WN, Bishop-Stewart J, Gray D, Johnson I. Chemical and physiological characterization of fluo-4 Ca^{2+}-indicator dyes. Cell Calcium 2000;27:97–106. [PubMed: 10756976]
16. Hund TJ, Rudy Y. Determinants of excitability in cardiac myocytes: mechanistic investigation of memory effect. Biophys J 2000;79:3095–3104. [PubMed: 11106615]
17. Huser J, Bers DM, Blatter LA. Subcellular properties of $[Ca^{2+}]_i$ transients in phospholamban-deficient mouse ventricular cells. Am J Physiol Heart Circ Physiol 1998;274:H1800–H1811.
18. Huser J, Blatter LA, Lipsius SL. Intracellular Ca^{2+} release contributes to automaticity in cat atrial pacemaker cells. J Physiol 2000;524:415–422. [PubMed: 10766922]
19. Janse, MJ.; Downar, E. Reentry. In: Spooner, PM.; Rosen, MR., editors. Foundations of Cardiac Arrhythmias: Basic Concepts and Clinical Approaches. Vol. chapt. 17. New York: Dekker; 2001.
20. Janse MJ, van Capelle FJ. Electrotonic interactions across an inexcitable region as a cause of ectopic activity in acute regional myocardial ischemia. A study in intact porcine and canine hearts and computer models. Circ Res 1982;50:527–537. [PubMed: 7067060]
21. Joyner RW, Wang YG, Wilders R, Golod DA, Wagner MB, Kumar R, Goolsby WN. A spontaneously active focus drives a model atrial sheet more easily than a model ventricular sheet. Am J Physiol Heart Circ Physiol 2000;279:H752–H763. [PubMed: 10924075]
22. Kaneko T, Tanaka H, Oyamada M, Kawata S, Takamatsu T. Three distinct types of Ca^{2+} waves in Langendorff-perfused rat heart revealed by real-time confocal microscopy. Circ Res 2000;86:1093–1099. [PubMed: 10827140]
23. Kimura H, Oyamada Y, Ohshika H, Mori M, Oyamada M. Reversible inhibition of gap junctional intercellular communication, synchronous contraction, and synchronism of intracellular Ca^{2+} fluctuation in cultured neonatal rat cardiac myocytes by heptanol. Exp Cell Res 1995;220:348–356. [PubMed: 7556443]
24. Laurita KR, Singal A. Mapping action potentials and calcium transients simultaneously from the intact heart. Am J Physiol Heart Circ Physiol 2001;280:H2053–H2060. [PubMed: 11299206]
25. Lipp P, Niggli E. Modulation of Ca^{2+} release in cultured neonatal rat cardiac myocytes. Insight from subcellular release patterns revealed by confocal microscopy. Circ Res 1994;74:979–990. [PubMed: 8156645]
26. Lipsius SL, Huser J, Blatter LA. Intracellular Ca^{2+} release sparks atrial pacemaker activity. News Physiol Sci 2001;16:101–106. [PubMed: 11443225]
27. Lukyanenko V, Subramanian S, Gyorke I, Wiesner TF, Gyorke S. The role of luminal Ca^{2+} in the generation of Ca^{2+} waves in rat ventricular myocytes. J Physiol 1999;518:173–186. [PubMed: 10373699]
28. Martinez-Zaguilan R, Parnami G, Lynch RM. Selection of fluorescent ion indicators for simultaneous measurements of pH and Ca^{2+} Cell Calcium 1996;19:337–349. [PubMed: 8983854]
29. Meiry G, Reisner Y, Feld Y, Goldberg S, Rosen M, Ziv N, Binah O. Evolution of action potential propagation and repolarization in cultured neonatal rat ventricular myocytes. J Cardiovasc Electrophysiol 2001;12:1269–1277. [PubMed: 11761415]
30. Michaels DC, Chialvo DR, Matyas EP, Jalife J. Dynamics of synchronization in the sinoatrial node. Ann NY Acad Sci 1990;591:154–165. [PubMed: 2197918]

31. Mohabir R, Ferrier GR. Effects of ischemic conditions and reperfusion on depolarization-induced automaticity. Am J Physiol Heart Circ Physiol 1988;255:H992–H999.
32. Morley GE, Ek-Vitorin JF, Taffet SM, Delmar M. Structure of connexin43 and its regulation by pH_i. J Cardiovasc Electrophysiol 1997;8:939–951. [PubMed: 9261721]
33. Nakamura T, Hayashi H, Satoh H, Katoh H, Kaneko M, Terada H. A single cell model of myocardial reperfusion injury: changes in intracellular Na^+ and Ca^{2+} concentrations in guinea pig ventricular myocytes. Mol Cell Biochem 1999;194:147–157. [PubMed: 10391134]
34. Pertsov AM, Davidenko JM, Salomonsz R, Baxter WT, Jalife J. Spiral waves of excitation underlie reentrant activity in isolated cardiac muscle. Circ Res 1993;72:631–650. [PubMed: 8431989]
35. Pogwizd SM. Nonreentrant mechanisms underlying spontaneous ventricular arrhythmias in a model of nonischemic heart failure in rabbits. Circulation 1995;92:1034–1048. [PubMed: 7543829]
36. Pogwizd SM, Corr B. The contribution of nonreentrant mechanisms to malignant ventricular arrhythmias. Basic Res Cardiol 1992;87:115–129. [PubMed: 1299206]
37. Pogwizd SM, Hoyt RH, Saffitz JE, Corr PB, Cox JL, Cain ME. Reentrant and focal mechanisms underlying ventricular tachycardia in the human heart. Circulation 1992;86:1872–1887. [PubMed: 1451259]
38. Post JA, Verkleij AJ, Langer GA. Organization and function of sarcolemmal phospholipids in control and ischemic/reperfused cardiomyocytes. J Mol Cell Cardiol 1995;27:749–760. [PubMed: 7776380]
39. Rohr S, Kucera JP, Fast VG, Kleber AG. Paradoxical improvement of impulse conduction in cardiac tissue by partial cellular uncoupling. Science 1997;275:841–844. [PubMed: 9012353]
40. Rohr S, Salzberg BM. Multiple site optical recording of transmembrane voltage (MSORTV) in patterned growth heart cell cultures: assessing electrical behavior, with microsecond resolution, on a cellular and subcellular scale. Biophys J 1994;67:1301–1315. [PubMed: 7811945]
41. Rosenthal JE, Ferrier GR. Contribution of variable entrance and exit block in protected foci to arrhythmogenesis in isolated ventricular tissues. Circulation 1983;67:1–8. [PubMed: 6847788]
42. Shaw RM, Rudy Y. Electrophysiologic effects of acute myocardial ischemia: a theoretical study of altered cell excitability and action potential duration. Cardiovasc Res 1997;35:256–272. [PubMed: 9349389]
43. Shaw RM, Rudy Y. Ionic mechanisms of propagation in cardiac tissue. Roles of the sodium and L-type calcium currents during reduced excitability and decreased gap junction coupling. Circ Res 1997;81:727–741. [PubMed: 9351447]
44. Starmer CF, Biktashev VN, Romashko DN, Stepanov MR, Makarova ON, Krinsky VI. Vulnerability in an excitable medium: analytical and numerical studies of initiating unidirectional propagation. Biophys J 1993;65:1775–1787. [PubMed: 8298011]
45. Swissa M, Qu Z, Ohara T, Lee MH, Lin SF, Garfinkel A, Karagueuzian HS, Weiss JN, Chen PS. Action potential duration restitution and ventricular fibrillation due to rapid focal excitation. Am J Physiol Heart Circ Physiol 2002;282:H1915–H1923. [PubMed: 11959659]
46. Takens-Kwak BR, Jongsma HJ, Rook MB, Van Ginneken AC. Mechanism of heptanol-induced uncoupling of cardiac gap junctions: a perforated patch-clamp study. Am J Physiol Cell Physiol 1992;262:C1531–C1538.
47. Tamaddon HS, Vaidya D, Simon AM, Paul DL, Jalife J, Morley GE. High-resolution optical mapping of the right bundle branch in connexin40 knockout mice reveals slow conduction in the specialized conduction system. Circ Res 2000;87:929–936. [PubMed: 11073890]
48. Vanden Hoek TL, Shao Z, Li C, Zak R, Schumacker PT, Becker LB. Reperfusion injury on cardiac myocytes after simulated ischemia. Am J Physiol Heart Circ Physiol 1996;270:H1334–H1341.
49. Wang Y, Rudy Y. Action potential propagation in inhomogeneous cardiac tissue: safety factor considerations and ionic mechanism. Am J Physiol Heart Circ Physiol 2000;278:H1019–H1029. [PubMed: 10749693]
50. Wang YG, Kumar R, Wagner MB, Wilders R, Golod DA, Goolsby WN, Joyner RW. Electrical interactions between a real ventricular cell and an anisotropic two-dimensional sheet of model cells. Am J Physiol Heart Circ Physiol 2000;278:H452–H460. [PubMed: 10666075]

51. White RL, Doeller JE, Verselis VK, Wittenberg BA. Gap junctional conductance between pairs of ventricular myocytes is modulated synergistically by H^+ and Ca^{++} J Gen Physiol 1990;95:1061–1075. [PubMed: 2115574]

52. Wilders R, Wagner MB, Golod DA, Kumar R, Wang YG, Goolsby WN, Joyner RW, Jongsma HJ. Effects of anisotropy on the development of cardiac arrhythmias associated with focal activity. Pflüers Arch 2000;41:301–312.

53. Winslow RL, Varghese A, Noble D, Adlakha C, Hoythya A. Generation and propagation of ectopic beats induced by spatially localized Na-K pump inhibition in atrial network models. Proc R Soc Lond B Biol Sci 1993;254:55–61.

54. Yamada KA, Saffitz JE, Corr PB. Role of alpha- and beta-adrenergic receptor stimulation in the genesis of arrhythmias during myocardial ischaemia. Eur Heart J 1986;7 Suppl A:85–90. [PubMed: 2873040]

55. Zaitsev AV, Berenfeld O, Mironov SF, Jalife J, Pertsov AM. Distribution of excitation frequencies on the epicardial and endocardial surfaces of fibrillating ventricular wall of the sheep heart. Circ Res 2000;86:408–417. [PubMed: 10700445]

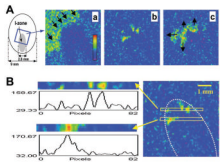

Fig. 1.

Generation of ectopic beats in the border zone. *A*: diagram on the *left* shows the experimental field and the injury zone (I-zone). The I-zone (shown in gray) was created by flows of control and ischemia-like solutions using a custom-designed superfusion chamber (2). Recordings of calcium transients (CaTs) were obtained from the border zone, inside the blue box shown on the *left*. The pseudocolor reflects increasing calcium concentrations as measured by fluo 4 fluorescence. *a*, Image was obtained during application of injury (I) solution. It shows a propagating wave of CaTs (CaT wave) that travels through the control area but does not penetrate into the I-zone. Black arrows point in the direction of CaT wave propagation. *b*, Appearance of ectopic clusters upon initiation of reperfusion. Three large clusters and a small one can be seen in this frame. *c*, Spreading of ectopic activity into surrounding network. Black arrows point in the direction of CaT wave propagation. *B: A*, *b* was used to plot the intensity profiles for regions where ectopic activity was observed. Two rectangular regions with their corresponding profiles are shown on the *left*. The position of these regions relative to the rest of the field can be seen on the *right*. The white dotted line marks the border of the I-zone.

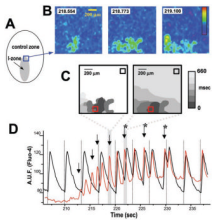

Fig. 2.

Progression of ectopic CaTs into arrhythmic episodes. *A*: diagram of the experimental field. Recordings from the border area inside the blue box are shown in *B* and were used to create the isochronal maps in *C*. *B*: initial stages of propagation of ectopic activity. Three consecutive images show the initial stages of ectopic cluster expansion. Elapsed time (in s) is shown in the boxes. The pseudocolor reflects increasing calcium concentrations. *C*: isochronal maps illustrating the growth and spread of ectopic activity. Each isochronal map is composed of several sequential frames (110 ms between frames) with the areas of increased intracellular calcium (Ca_i^{2+}) depicted in color. The colors correspond to the times shown on the *right*. The isochronal map on the *left* shows expansion of the ectopic activity presented in *B*. At that time (~219 s), the activity failed to spread into the surrounding cell network, and the event presented in this isochronal map is reflected as a distinct ectopic beat by the corresponding CaT trace. The following ectopic beats, including the one illustrated on the *right* isochronal map, propagated into the control network, causing an arrhythmia. *D*: CaTs collected from the control and ischemic areas (black and red squares in *C*). Dotted lines indicate timing of pacing stimuli. Initial 10 s of the recording shows that, during local ischemia, cells within the control network (black trace) exhibited regular CaTs, whereas cells within the I-zone were silent (red trace). Upon reperfusion, ectopic activity from the border zone (red trace, with arrows pointing to the individual beats) spread into the control network, causing an arrhythmia. *Additional peaks on the control trace between pacing stimuli, which were caused by the spread of ectopic activity from the border zone. Shaded regions correspond with the isochronal maps shown in *C*. AUF, arbitrary units of fluorescence.

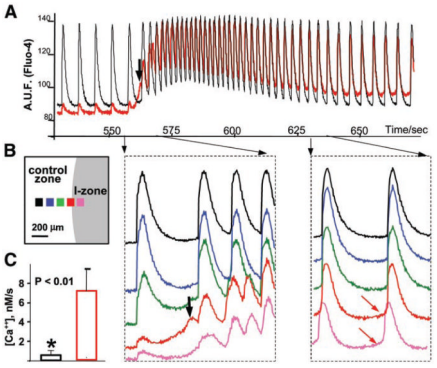

Fig. 3.

Changes in diastolic Ca_i^{2+} associated with ectopic activity. *A*: two traces from control (black) and border (red) zones illustrating an entire tachyarrhythmic episode are shown. Reperfusion was initiated at 550 s. The black arrow points to the first ectopic beat. *B*: relative position of the five regions of interest that used to acquire the traces on the *right*. The traces (shown in corresponding colors) reveal individual CaTs during the initial and late stages of the tachyarrythmic episode. The arrows point to the respective timing of the selected intervals.

The red arrows point to a positive slope in diastolic Ca_i^{2+} observed in ectopic regions. *C*: the averaged diastolic slope of CaTs from the ectopic regions (red column) was significantly greater ($P = 0.003$) than that from the control zone (black column). Fluo 4 fluorescence was converted to Ca_i^{2+}, as described in MATERIALS AND METHODS, to calculate these slopes.

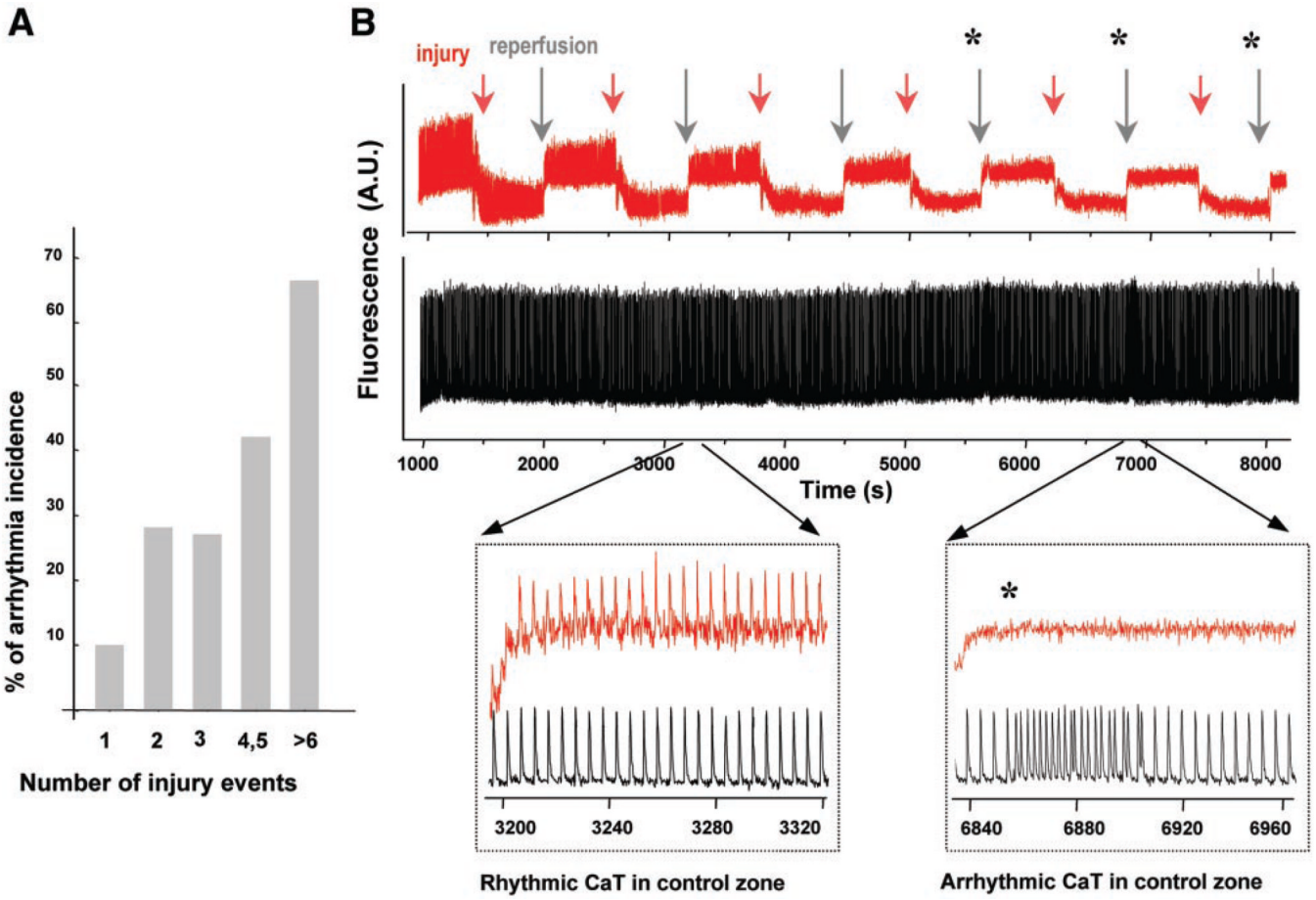

Fig. 4.

Repetitive injury increases the incidence of reperfusion arrhythmias. *A*: multiple brief superfusions with a heptanol-free ischemic solution increased the incidence of reperfusion arrhythmias in proportion to the number of injury events. Statistical data are from 35 experiments. *B, top*: continuous CaTs collected from the control zone (black) and I-zone (red) during six consecutive injury events, each consisting of 10 min of ischemia, followed by 10 min of reperfusion. The *top* traces are rather compressed and mainly illustrate changes in the relative amplitudes of CaTs. Acidic pH of the I-solution resulted in a downward shift of the fluo 4 baseline signal, due to its known pH dependence (28). The two *insets* below have an expanded time scale and reveal individual CaTs and changes in frequency. Specifically, the *left inset* shows that reperfusion after the second injury event recovers CaTs in the I-zone without changing the rhythmic control pattern. The *right inset* shows that reperfusion after the fifth injury event failed to restore CaTs inside the I-zone and induced an arrhythmia in the control zone. In this particular experiment, arrhythmic episodes occurred after the fourth, fifth, and sixth injury events (*).

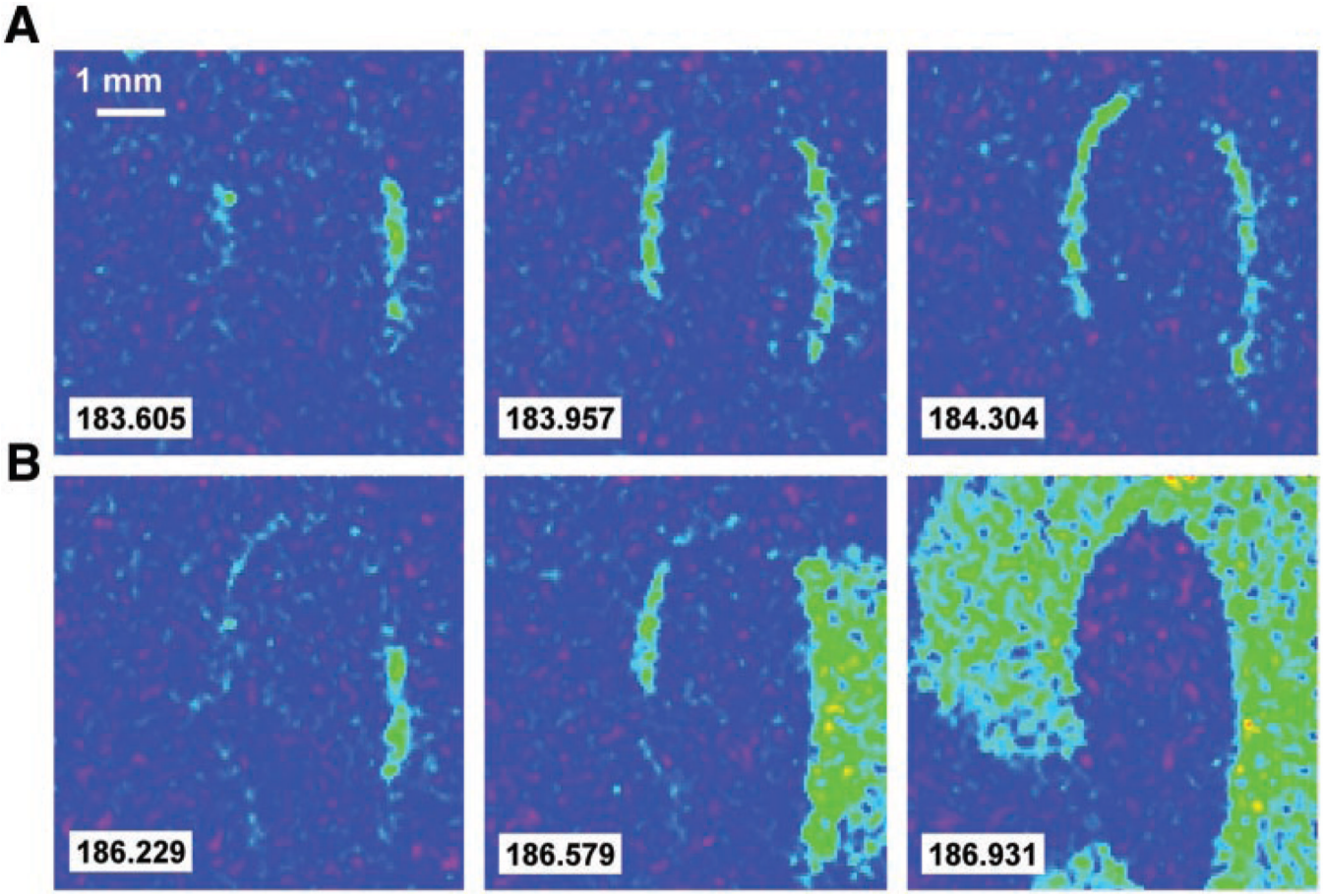

Fig. 5.

Border zone propagation. Consecutive frames illustrating the propagation of ectopic activity along the border zone during a microreperfusion protocol are shown. In this protocol, only a narrow, 300-μm width of border zone was reperfused with control Tyrode solution, whereas the remaining I-zone cells continued to be superfused with I-solution. *A*: microreperfusion caused the appearance of ectopic CaTs, which propagated alongside the border zone with an apparent speed of 0.1–0.4 cm/s. This sequence illustrates a wave of CaTs that receded without activating the surrounding control zone. *B*: spread of CaTs into the surrounding control network, where they were propagated at a faster velocity of 6–9 cm/s. A complete sequence of events can be seen in the online supplement.